PHYSICAL REVIEW D **83,** 063001 (2011)

Improved dark energy detection through the polarization-assisted cross correlation of the cosmic microwave background with radio sources

Guo-Chin Liu,[1] Kin-Wang Ng,[2,3] and Ue-Li Pen[4]

[1]*Department of Physics, Tamkang University, Tamsui, Taipei County, Taiwan 251, R.O.C.*
[2]*Institute of Astronomy and Astrophysics, Academia Sinica, Taipei, Taiwan 115, R.O.C.*
[3]*Institute of Physics, Academia Sinica, Taipei, Taiwan 115, R.O.C.*
[4]*Canadian Institute for Theoretical Astrophysics, University of Toronto, 60 St. George Street, Toronto, ON M5S 3H8, Canada*
(Received 1 September 2010; published 2 March 2011)

Integrated Sachs-Wolfe (ISW) effect can be estimated by cross-correlating the cosmic microwave background (CMB) sky with tracers of the local matter distribution. At late cosmic time, the dark energy–induced decay of gravitation potential generates a cross correlation signal on large angular scales. The dominant noise is the intrinsic CMB anisotropies from the inflationary epoch. In this paper we use CMB polarization to reduce this intrinsic noise. We cross-correlate the microwave sky observed by Wilkinson Microwave Anisotropy Probe (WMAP) with the radio source catalog compiled by NRAO VLA Sky Survey (NVSS) to study the efficiency of the noise suppression. We find that the error bars are reduced by about 4 to 14% and the statistical power in the signal is improved.

DOI: 10.1103/PhysRevD.83.063001 PACS numbers: 98.70.Vc, 95.36.+x, 98.80.Es

I. INTRODUCTION

Recently released data made by the Wilkinson Microwave Background Probe (WMAP) [1] are used to study different cosmological models with an unprecedented accuracy. The observed data put tight constraints on intrinsic properties of the Universe such as geometry, matter content, the origin of inhomogeneities, and the formation of large-scale structures. Furthermore, combining WMAP data with observations of type Ia supernovae [2] and large-scale structures (e.g., in Ref. [3]) makes our understanding of the Universe converge to a concordance model. In this model, the present Universe, dominated by dark energy with negative pressure, is accelerating at late times. Although dark energy can explain the acceleration, we know very little about its nature and origin. More observations are definitely necessary for constraining this dark energy component.

As CMB photons propagate through a gravitational potential generated by large-scale structures in the expanding Universe, the photons undergo an energy shift. In a matter-dominated universe, the gravitational potential stays constant, so the CMB temperature fluctuations generated through this so-called Sachs-Wolfe (SW) effect [4] depend only on the potential difference between the recombination epoch and the present time. However, the existence of a spatial curvature or dark energy results in a time-varying gravitational potential, thus producing, in addition to the SW effect, time-integrated temperature fluctuations of the CMB. This is known as the integrated Sachs-Wolfe (ISW) effect [4]. Therefore, the detection of the late-time ISW effect in a flat universe can be regarded as a direct dynamical evidence for dark energy. Furthermore, measuring the ISW effect provides an independent method to probe the properties of dark energy.

The ISW effect manifests itself on large angular scales because the CMB temperature fluctuations or anisotropies are dominantly induced by the gravitational potential at large scales. On these angular scales, the CMB signal is dominated by the primary anisotropies generated from the recombination epoch at redshift $z \simeq 1100$ as well as from the reionization epoch at redshift $z \simeq 10$. It is not easy to isolate the ISW effect from the primary CMB fluctuations. In addition, the precision of the large-scale anisotropy measurement is limited by the unavoidable cosmic variance. Therefore, attempts at measuring the ISW effect solely from CMB experiments may not be able to give significant constraints on dark energy models.

However, a positive large-scale correlation signal may occur by correlating the CMB sky with the local matter distribution as a result of the ISW effect. This idea was first explored by Crittenden and Turok [5]. Several authors tried to detect the ISW effect by correlating CMB satellite data with different matter tracers. The CMB anisotropy data made by the Cosmic Background Explorer (COBE) was firstly used for this study [6]. However, the authors concluded that the resolution and sensitivity of COBE were not good enough for a detection. Recently, the WMAP mission has provided a set of high-quality CMB data. As to the matter distribution, several tracers have been used for this study, such as radio sources provided by NRAO VLA Sky Survey (NVSS) [7], hard x-ray data from the High Energy Astronomy Observatory-1 satellite (HEAO-1) [8], Sloan Digital Sky Survey (SDSS) data [9], and Two Micron All Sky Survey Extended Source Catalog (2MASS XSC) [10]. Douspis *et al.* [11] and Frommert *et al.* [12] have investigated the properties of a survey required to detect this correlated signal. The data analyses of the cross correlation are performed in real [6,13,14], harmonic [15], and wavelet [16,17] spaces.

A significant uncertainty in the cross correlation is coming from the spurious correlation of matter distribution with the primary CMB anisotropies generated from the recombination and reionization epochs. It plays a role like the cosmic variance in observations of the low multipoles of the CMB anisotropy that have only a few independent modes. This spurious correlation obscures the measurement of the true correlation that we are interested in and indeed weakens the constraint on the dark energy component. However, CMB polarization is also generated when the primary anisotropies are scattered by free electrons in these two epochs. Using the fact that the ISW effect occurs at relatively late times, the information imprinted on the CMB polarization may give an opportunity to separate the ISW effect from the primary anisotropies. If this can be done, we will suppress or even get rid of the spurious correlation. Here, we construct a simple relation between the CMB polarization and its corresponding primary anisotropies. This relation is found to be weakly dependent on the emerging dark energy at late times, thus allowing us to subtract the primary CMB anisotropies from the CMB anisotropy data to obtain the genuine ISW signal. Then, the resulting anisotropies are used to correlate with matter tracers to obtain a better signal-to-noise detection of the cross correlation.

II. LARGE-SCALE ANISOTROPY-POLARIZATION CORRELATION

Instead of using Stokes parameters Q and U [18], CMB polarization is conventionally characterized by a curl-free component, commonly called the E mode, and a divergence-free component, the B mode. Small-scale polarization of the CMB is generated through Thomson scattering of the CMB anisotropic radiation by free electrons at the recombination epoch. For the angular scales at which the cross-correlated ISW effect is concerned, E-mode polarization is generated by rescattering off the free electrons at reionization epoch, and B-mode polarization is also generated in the presence of tensor-mode perturbations, predicted, for example, in inflation model. So far, there is no evidence for the B-mode polarization, so we will not consider it.

Since CMB polarization is generated from temperature anisotropies, we expect some relation between the E-mode polarization and the CMB anisotropies. We simply assume that the relation can be written as

$$a_{E,\ell m}^{\mathrm{NOISW}} = r_\ell a_{T,\ell m}^{\mathrm{NOISW}} + n_\ell. \quad (1)$$

Here $a_{E,\ell m}^{\mathrm{NOISW}}$ and $a_{T,\ell m}^{\mathrm{NOISW}}$ are the coefficients of E-mode polarization and temperature anisotropies in spherical harmonics space, and the coefficient r_ℓ gives us the idea how much the correlation of E-mode polarization with temperature anisotropies and n_ℓ plays a role like the ''noise'' of this relation. For our purpose, we construct this relation in the situation in which the ISW effect is removed.

We define the ''E-mode polarization-corrected '' temperature anisotropies as

$$\tilde{a}_{T,\ell m} = a_{T,\ell m} - a_{E,\ell m}/r_\ell \simeq a_{T,\ell m} - a_{E,\ell m}^{\mathrm{NOISW}}/r_\ell. \quad (2)$$

We have made the approximation in the last equality because of the fact [19,20] that the polarization contributed by the ISW effect is significantly smaller than that contributed by rescattering of the primary temperature quadrupole in the reionization. Then, we cross-correlate $a_{E,\ell m}^{\mathrm{NOISW}}$ in Eq. (1) with the CMB temperature anisotropies:

$$\langle a_{T,\ell m}^* a_{E,\ell m}\rangle^{\mathrm{NOISW}} = r_\ell \langle a_{T,\ell m}^* a_{T,\ell m}\rangle^{\mathrm{NOISW}}, \quad (3)$$

and obtain the autocorrelation as

$$\langle a_{E,\ell m}^* a_{E,\ell m}\rangle^{\mathrm{NOISW}} = r_\ell^2 \langle a_{T,\ell m}^* a_{T,\ell m}\rangle^{\mathrm{NOISW}} + n_\ell^2. \quad (4)$$

The ensemble averages of $\langle a_{T,\ell m}^* a_{T,\ell m}\rangle$, $\langle a_{T,\ell m}^* a_{E,\ell m}\rangle$, and $\langle a_{E,\ell m}^* a_{E,\ell m}\rangle$ are used to define the power spectra $C_{T\ell}$, $C_{C\ell}$, and $C_{E\ell}$, respectively. Thus, we can calculate the r_ℓ and n_ℓ for each multipole using Eqs. (3) and (4), given the power spectra $C_{T\ell}$, $C_{C\ell}$, and $C_{E\ell}$ from the theoretical prediction. In practice, we use the power spectra obtained from running the CMBFAST code [21] with the WMAP best-fit cosmological parameters. We modify the code to remove the ISW effect by forcing the time-varing gravitational to vanish for redshift $z < 5$. Once the r_ℓ and n_ℓ are determined, they can be applied to real data. However, in numerical practice, we have found that the numbers r_ℓ are quite small due to the fact that $C_{C\ell}$ are typically 2 orders of magnitude smaller than $C_{T\ell}$. Therefore, the noise term n_ℓ^2 obtained from Eq. (4) is in fact comparable to $\langle a_{E,\ell m}^* a_{E,\ell m}\rangle$. It means that $a_{T,\ell m} - a_{E,\ell m}/r_\ell$ may result in an oversubtraction due to the noise n_ℓ. To circumvent this

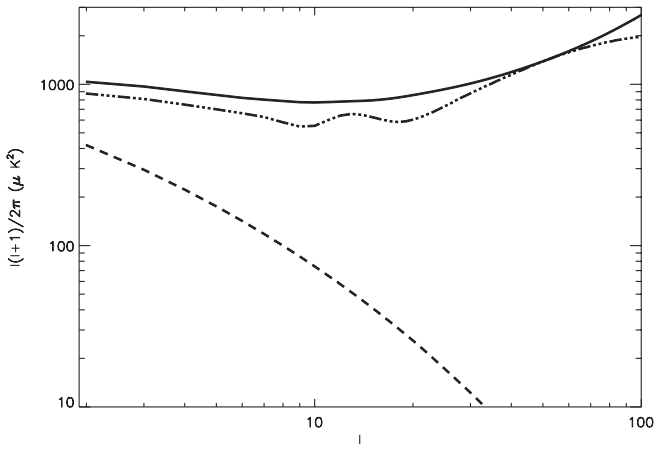

FIG. 1. Power spectrum of the CMB temperature anisotropies after the correction by the E-mode polarization (dot-dashed curve). For comparison, we also plot the total power spectrum before correction (solid curve) and the ISW effect (dashed curve). Using information from the anisotropy-polarization correlation, we can filter out the part of the signal coming from redshifts before $z = 5$.

problem, we multiply each $a_{E,\ell m}/r_\ell$ by a Wiener filter constructed as

$$W_{1\ell} = \langle a^*_{T,\ell m} a_{T,\ell m}\rangle / (\langle a^*_{T,\ell m} a_{T,\ell m}\rangle + n^2_\ell / r^2_\ell). \quad (5)$$

In Fig. 1, we plot the E-mode polarization-corrected power spectrum (denoted by the dot-dashed curve) of the temperature anisotropies, $C_{\tilde{T}\ell} = \langle \tilde{a}^*_{T,\ell m} \tilde{a}_{T,\ell m}\rangle$, where $\tilde{a}_{T,\ell m}$ is defined in Eq. (2). To simulate $a_{T,\ell m}$ and $a_{E,\ell m}$, we have generated 9000 CMB sky maps, using the power spectra with the total power of the temperature anisotropies, which is plotted in Fig. 1 by the solid curve. For comparison, we also plot the isolated ISW effect denoted by the dashed curve. We have found that we can filter out more than about 10% of the primary temperature anisotropies for the multipoles $\ell < 30$. For $40 < \ell < 70$, the correction is inefficient due to the low anisotropy-polarization correlation in the theoretical prediction. More efficient correction occurs for $80 < \ell < 100$ (as shown in Fig. 1); however, the cross correlation signal of the CMB and large-scale structure is small at this angular scale [5].

III. APPLYING TO WMAP AND NVSS DATA

Now we apply the "corrected" temperature anisotropies described above to calculate their cross correlation with the matter tracers. We use the WMAP 7-year foreground reduced maps with full resolution. We take only the Q and V frequency channels because of the low contamination from the foreground emission on both temperature anisotropies and polarization [1]. For the matter distribution, we use NVSS radio sources. NVSS is operated at 1.4 GHz with flux limit 2.5 mJy. It is complete for declination $\delta > -40°$ and contains 1.8×10^6 sources. Its 82% sky coverage provides good information on large angular scales. Though the redshifts of individual radio sources are largely unknown, the luminosity function [22] indicates that they are distributed in redshift range $0 < z < 2$, with a peak distribution at $z \sim 0.8$. Boughn and Crittenden [6,13] have studied the signal contribution of the cross correlation with different cutoffs in redshift and concluded that the redshift distribution of the NVSS radio sources is very suitable for this study. The cross correlation power spectrum between NVSS and WMAP is simply calculated by

$$C^{NW}_\ell = \frac{1}{2\ell+1} \sum_m \langle a^N_{\ell m} a^{*W}_{\ell m}\rangle, \quad (6)$$

where $a^N_{\ell m}$ and $a^W_{\ell m}$ are the harmonic coefficients of the NVSS and WMAP maps, respectively. We distribute the NVSS catalog in the Healpix scheme [23] at the resolution-9 map, whose resolution is the same with the WMAP 7-year foreground reduced maps. Such a map has $12N_{\rm side}$ pixels with the same area in all sky, where $N_{\rm side} = 2^9$. We calculate the coefficients of the spherical harmonics a_{lm} for the temperature anisotropies, the E-mode polarization, as well as the NVSS sources, using the HEALPIX package with a mask which is obtained by combining the standard polarization mask (P06) used by the WMAP team and the blank sky of the NVSS survey. Applying this mask gives a sky coverage of about 56% and the average number density of NVSS radio galaxies is $171494/sr$.

IV. RESULTS

In Fig. 2, we plot the signal of the cross correlation of WMAP and NVSS for the Q and V frequency bands with error bars obtained by cross-correlating 9000 simulated CMB sky maps with the NVSS catalog. From the covariance matrix computed from 9000 simulations, we found that masking about 44% of the sky would cause about 40% correlation among neighboring multipoles. To reduce the correlation among neighboring multipoles, we bin our results into five bins with equal spaces in logarithm-ℓ from 2 to 100 using the well-known minimum-variance method $\mathbf{N_p} = (\mathbf{A}^T \mathbf{N}^{-1} \mathbf{A})^{-1}$ [24], where $\mathbf{N}$ is the 99×99 covariance matrix from 9000 simulations, and $\mathbf{N_P}$ is the 5×5 binned covariance matrix. The 99×5 point matrix $\mathbf{A}$ is defined with matrix elements that $A_{ij} = 1$ if the ith multipole lies in the jth band, otherwise $A_{ij} = 0$. We tabulate the correlation coefficients of the binned covariance matrix in Table I.

The instrumental noise in the WMAP data at such large angular scales is negligible when compared to temperature anisotropies, but it is comparable to the E polarization signal. Therefore, in practice, we find the *estimated* ISW temperature as

$$\tilde{a}_{T,\ell m} = a_{T,\ell m} - W_{1\ell} W_{2\ell} a^{\rm NOISW}_{E,\ell m} / r_\ell, \quad (7)$$

with one more Wiener filter given by

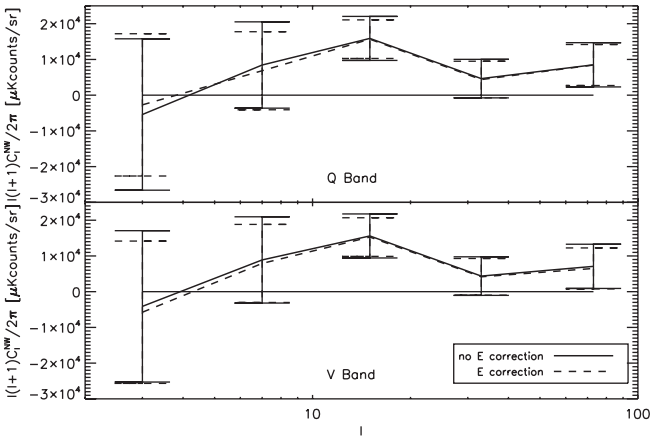

FIG. 2. cross correlation of WMAP and NVSS for Q and V frequency bands. The error bars are calculated by cross-correlated 9000 simulated CMB skies with NVSS catalog. Using E-polarization, the error bars and signal of cross correlation are changed.

TABLE I. Correlation coefficient matrix from the 9000 simulated band power before/after the correction by the E-mode polarization.

1	0.237/0.228	0.112/0.110	$5.39 \times 10^{-2}/5.31 \times 10^{-2}$	$6.68 \times 10^{-2}/6.59 \times 10^{-2}$
	1	0.103/0.106	$2.52 \times 10^{-2}/2.65 \times 10^{-2}$	$1.60 \times 10^{-2}/1.38 \times 10^{-2}$
		1	0.135/0.138	$5.09 \times 10^{-2}/5.09 \times 10^{-2}$
			1	$4.40 \times 10^{-2}/4.40 \times 10^{-2}$
				1

$$W_{2\ell} = \langle a^*_{E,\ell m} a_{E,\ell m} \rangle / (\langle a^*_{E,\ell m} a_{E,\ell m} \rangle + N_\ell), \quad (8)$$

where N_ℓ is the noise power spectrum of the covariance matrix N for the instrumental noise. We have calculated N from the thermal noise in each pixel provided by the WMAP team without taking into account the correlated noise between different pixels. It may cause the wrong power estimation in low-ℓ multipoles. Also, we need to notice that we cannot obtain the exact values of the multipoles by this method due to the incomplete coverage of the sky. In case of modelling or parameter fitting, we need to estimate these two factors carefully.

The spurious correlation resulting from the primary CMB temperature anisotropies can be quantified using simulated, uncorrelated CMB maps. We use the 9000 simulated CMB sky maps in the previous section to do the blind correlation with the real NVSS data. The error bars in Fig. 2 show the 1σ region derived from this result. Let us define $\chi^2 = \sum_{i,j} (\hat{C}_{Bi} - C_{Bi}) N^{-1}_{p,ij} (\hat{C}_{Bj} - C_{Bj})$, where $\hat{C}_{Bi}$ and C_{Bi} are, respectively, the measured and predicted band powers of the WMAP-NVSS cross correlation. For a model with null correlation, i.e., $C_{Bi} = 0$, we find that $\chi^2 = 7.63$ for the Q band and $\chi^2 = 7.04$ for the V band in the case without the E-polarization correction. After the E-polarization correction, the values increase to $\chi^2 = 9.18$ for the Q band and $\chi^2 = 8.39$ for the V band. Our fit yields an ISW signal of 2.76σ and 2.65σ for the Q and V band, respectively. The E-polarization correction improves the signal to 3.03σ for the Q band and 2.90σ for the V band. We also find that the correction improves the errors resulted from the spurious correlation by 8.15%, 13.6%, 12.9%, 8.0%, and 3.9% in the five respective bins.

ACKNOWLEDGMENTS

After finishing this work, we found that the idea about the improvement of the ISW detection by use of CMB polarization data was initially proposed by R. Crittenden, following a suggestion from L. Page [25], and has been worked out by M. Frommert and T. A. Ensslin [26]. However, this is the first paper to apply the technique to real data. We acknowledge the WMAP science team for the use of data from the WMAP satellite and the authors of Ref. [7] for the use of the NVSS catalog. G. C. Liu appreciates the discussions with N. Aghanim and M. Douspis for the galaxy surveys for ISW detection and L. Chiang for fruitful discussions on the WMAP data. G. C. Liu and K. W. Ng are thankful for support from the National Science Council of Taiwan under Grants No. NSC97-2112-M-032-007-MY3 (NSC98-2112-M-001-009-MY3) and from the Institute of Physics, Academia Sinica.

[1] N. Jarosik *et al.*, Astrophys. J. Suppl. Ser., **192** 14 (2011).
[2] R. A. Knop *et al.*, Astrophys. J. **598**, 102 (2003).
[3] S. W. Allen, R. W. Schmidt, and A. C. Fabian, Mon. Not. R. Astron. Soc. **334**, L11 (2002).
[4] R. K. Sachs and A. M. Wolfe, Astrophys. J. **147**, 73 (1967).
[5] R. G. Crittenden and N. Turok, Phys. Rev. Lett. **76**, 575 (1996).
[6] S. P. Boughn and R. G. Crittenden, Phys. Rev. Lett. **88**, 021302 (2001).
[7] J. J. Condon, W. D. Cotton, E. W. Greisen, Q. F. Yin, R. A. Perley, G. B. Taylor, and J. J. Broderick, Astron. J. **115**, 1693 (1998).
[8] E. Boldt, Phys. Rep. **146**, 215 (1987).
[9] D. G. York *et al.*, Astron. J. **120**, 1579 (2000).
[10] T. H. Jarrett, T. Chester, R. Cutri, S. Schneider, M. Skrutskie, and J. P. Huchra, Astron. J. **119**, 2498 (2000).
[11] M. Douspis, P. G. Castro, C. Caprini, and N. Aghanim, Astron. Astrophys. **485**, 395 (2008).
[12] M. Frommert, T. A. Ensslin, and F. S. Kitaura, Mon. Not. R. Astron. Soc. **391**, 1315 (2008).
[13] S. P. Boughn and R. G. Crittenden, Nature **427**, 45 (2004).
[14] M. R. Nolta *et al.*, Astrophys. J. **608**, 10 (2004).
[15] N. Afshordi, Y. S. Loh, and M. A. Strass, Phys. Rev. D **69**, 083542 (2004).
[16] P. Vielva, E. Martinez-Gonzalez, and M. Tucci, Mon. Not. R. Astron. Soc. **365**, 891 (2006).
[17] J. D. McEwen, Y. Wiaux, M. P. Hobson, P. Vandergheynst, and A. N. Lasenby, Mon. Not. R. Astron. Soc. **384**, 1289 (2008).
[18] S. Chandrasekar, *Radiative Transfer* (Dover, New York, 1960).

[19] K. W. Ng, in *Proc. of the 1st RESCEU Int. Symp., Cosmological Constant and the Evolution of the Universe*, edited by K. Sato, T. Suginohara, and N. Sugiyama (Universal Academy Press, Tokyo, 1996), p. 31.
[20] A. Cooray and A. Melchiorri, J. Cosmol. Astropart. Phys. 01 (2006) 018.
[21] U. Seljak and M. Zaldarriaga, Astrophys. J. **469**, 437 (1996).
[22] J. S. Dunlop and J. A. Peacock, Mon. Not. R. Astron. Soc. **247**, 19 (1990).
[23] K. M. Gorski, E. Hivon, A. J. Banday, B. D. Wandelt, F. K. Hansen, M. Reinecke, and M. Bartelmann, Astrophys. J. **622**, 759 (2005).
[24] M. Tegmark, Astrophys. J. **480**, L87 (1997).
[25] R. Crittenden, see http://www-astro-theory.fnal.gov/Conferences/ECcmbC/PresentationFiles/RobertCrittenden.ppt and http://www-astro-theory.fnal.gov/Conferences/ECcmbC/ECcmbCagenda.html.
[26] M. Frommert and T. A. Ensslin, Mon. Not. R. Astron. Soc. **395**, 1837 (2009).